2017 IEEE International Conference on Robotics and Automation (ICRA)
Singapore, May 29 - June 3, 2017

Toward Robust, Whole-hand Caging Manipulation with Underactuated Hands

Raymond R. Ma, *Student Member, IEEE,* Walter G. Bircher, *Student Member, IEEE,*
and Aaron M. Dollar, *Senior Member, IEEE*

***Abstract*— Human in-hand dexterity can be highly fluid and unstructured, but in contrast, prevailing research in robotic manipulation has focused on highly structured, well-controlled motions where contact points are carefully characterized. Maintaining grasp stability through traditional closure conditions during complex within-hand manipulation motions can be difficult, even with highly-articulated end-effectors. However, simple grippers can still achieve an effective range of in-hand manipulation tasks without strict closure conditions, as long as the object can be bounded locally relative to the hand frame. The end-effector can be utilized as a tool to limit the range of possible object poses. We show that the hand-object system's configuration space can be sampled to find a set of manipulation primitives that can reliably constrain the object inside the hand workspace even without feedback, a strategy proposed as *whole-hand caging manipulation*. Experimental results with a planar (gravity into the page), two-finger underactuated gripper (Yale OpenHand) are presented to validate this manipulation strategy, and it is shown that even though contacts are regularly broken and reformed, the object can be repeatability manipulated within the hand workspace without ejection, enabling challenging behaviors such as sliding and gaiting.**

***Index Terms*—dexterous manipulation, caging, whole-hand manipulation, open-loop**

I. Introduction

Traditionally, within-hand manipulation has been modeled as a set of independently controlled fingers applying some controlled load, or wrench, to the object through point contacts. The fingers, usually represented as fully-actuated serial chains, are coordinated such that the desired stability and closure conditions are maintained as the system modulates the object pose [1], [2]. Despite extensive study in this area, physical implementations of dexterity with robotic hands has remained a major challenge, even with recent advances in hardware [3] and control fidelity [4], due to the high degree of sensing and control complexity that this approach requires.

However, in-hand dexterity is not necessarily restricted to manipulation with fingertips exclusively [5], nor do hands need to always maintain closure conditions throughout the commanded task [6]. Consider the task of picking a screwdriver out of a cluttered bin and re-orienting it properly into a secure grip for use. As the screwdriver is transitioned into the desired grasp, the number and nature of the contacts may change frequently, and there are likely many transitionary instances where even a small external wrench would be enough to eject the tool from the hand. It can be argued that the task is considered successful as long as the screwdriver can eventually be secured into the desired grasp.

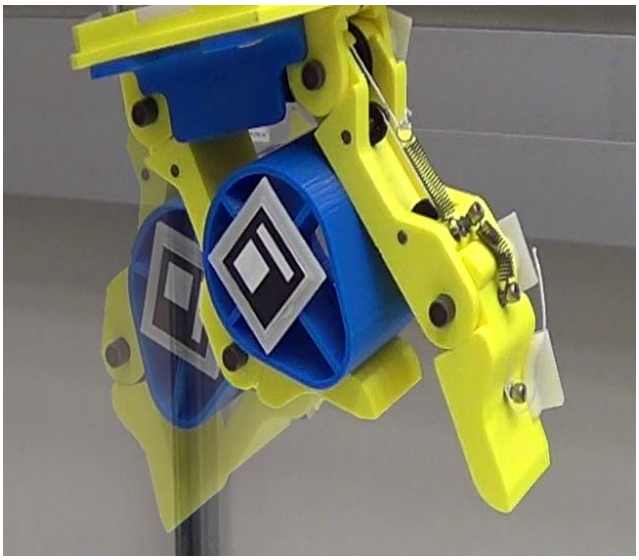

Fig. 1 – Whole-hand caging manipulation with an underactuated robotic hand.

We propose that ensuring repeatable object motion to an adequate range of poses for a set of system inputs can be a sufficient form of in-hand dexterity. The manner in which the object reaches the target pose or how the contact conditions change, disengage, and re-establish is not critical. By relaxing some of the constraints and requirements in traditional manipulation, other useful and simpler control strategies can be explored. As shown in Fig. 1, minimalist hands with simple control schemes can produce in-hand object motion.

Caging has been proposed as a robust method to bound the permissible range of poses for an object, albeit predominantly in the context of mobile, distributed robotics in the plane [7]. This approach simplifies the control scheme by permitting a limited amount of object free motion, recognizing that the system does not need to fully constrain the object during every phase of the task. Researchers have recently begun to acknowledge the potential utility for robotic hands performing caging primitives [8]–[11], but to our knowledge, none have evaluated this strategy for in-hand manipulation with physical robotic grippers.

In this paper, we detail the concept of whole-hand manipulation via caging, or *caging manipulation*, a dexterous control strategy especially well-suited for simple and/or underactuated grippers. Simple hands with a limited number of actuators can be configured such that even in the

TABLE I
OBJECT ENERGY FIELD METHODOLOGY PSEUDOCODE

```
For each hand configuration q_hand:
    If isCaging(q_hand), S_caging ← q_hand
For each caging hand configuration q_caging ∈ S_caging
    For each actuated component AC_j:
        Calculate object contact subspace CS_j(q_caging)
    Add ∩_j^P CS_j(q_caging), q_caging to object contact space
    OC
For each q_obj, q_caging ∈ OC:
    Calculate E_A(q_caging)
    Add q_obj, min(E_A(q_caging), EO(q_obj)) to object energy
    field EO
```

absence of force or form closure conditions, the object configuration space can be adequately limited and localized. This approach allows for robust open-loop control and can be shown to produce highly repeatable results without needing to characterize or track the contact conditions. Passive grasp adaptability through underactuated design can then be leveraged to further constrain the object after manipulation completes. This control methodology only requires the object to start within a local *capture region* [12] in the hand workspace, not any particular precision or power-grasp configurations, and it does not require any coordination between contact points. Extensive experimental results from the implementation of a planar underactuated hand and several object geometries will be presented to demonstrate the efficacy of this approach.

II. CAGING MANIPULATION MODEL

The manipulation strategy described in this paper combines previous work done on caging with linkage-based grippers [8], [9] and energy-based evaluation of underactuated hands' ability to hold and localize an object [13], [14]. An ideal, unconstrained object alone can be freely moved in its configuration space without any additional energy. Obstacles that are introduced into the object configuration space reduce its free workspace, and a hand can be thought of as a collection of rigid and compliant obstacles relative to the object that restricts its free space. Table I summarizes a methodology used to determine a hand's caging manipulation capability

Unlike the traditional notion of caging, which assumes static obstacles that generate fixed, inaccessible regions in the object workspace, we recognize that actuated components, such as finger phalanges and gripper surfaces, have an associated energy state [13], [14] that changes depending on their interactions with the object and other components in the system. Evaluating the energy state of the full hand-object system is a useful way to analyze how the multiple actuated components affect the object pose stability and motion.

In the absence of an object or other components, an actuated component in a conservative system should resolve to the lowest possible energy state. For example, a finger actuated with a constant torque input will attempt to close

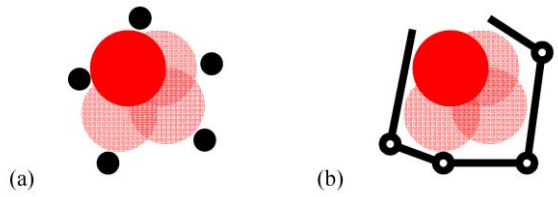

Fig. 2 – Manipulated object (shown in red) can be caged via point obstacles (a) or hand/gripper components (b)

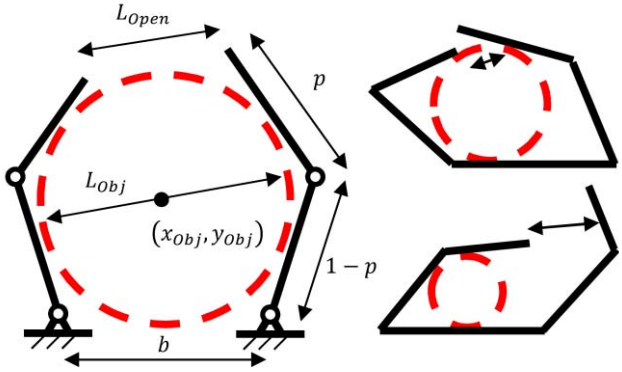

Fig. 3 - The caging capability of a planar hand configuration can be efficiently approximated by the largest inscribed circle with diameter L_{obj} and the smallest escape opening length L_{open} of the grasp polygon: the region bounded by the hand components.

fully, until it contacts an obstacle that restricts its motion or reaches a physical hard-stop. A system with multiple actuated components is expected to reconfigure toward the overall energy-minimal configuration that satisfies the necessary kinematic limits.

With respect to caging, there may be multiple energy-minimal system configurations for a given set of actuation inputs. However, for any given set of inputs, we can identify a stable *attractor region* in the object workspace toward which the manipulator is actively driving the object.

A. Caging Condition

In summary, an object is caged if it cannot be moved to a point at infinity without intersecting other components in its workspace. Fig. 2 compares the traditional caging problem, commonly utilizing point-based obstacles, and the corresponding caging problem for a planar, two-finger hand, which can be represented by a set of serial chains. The generalized caging problem has been previously detailed and thoroughly investigated by several researchers [8], [11], [15].

For the simplified planar case, which will be the focus of this paper, the caging problem can be simplified to two sub-problems regarding the *grasp polygon*: finding the minimum opening length L_{Open} and the diameter of the maximal inscribed circleL_{Obj}, as detailed in Fig. 3. The grasp polygon is the planar polygon with edges formed by the finger phalanges, the palm surface, and the edge between the pair of distal fingertips. For the common case with two opposition fingers, the minimal opening can be found as either the magnitude of the vector between the distal fingertips or the vector between a distal fingertip and an

opposing phalanx, perpendicular to that phalanx. The maximal inscribed circle is found by iterating through all unique triplets of grasp polygon edges and finding the circles tangent to all three edges with centers lying within the grasp polygon. The resulting set of configurations S_{caging} is an approximation of the hand's caging capability and greatly reduces the number of system configurations that need to be evaluated for each object geometry.

B. Caged-Object-Contact Space

It is more computationally efficient to focus our investigation of the hand-object system to the *caged object-contact space*, the set of object-hand configurations where the hand cages the object and work is being done on the actuators due to object contact during manipulation. Though the analysis presented here will also account for configurations where the object does not necessarily make contact with the hand components, physical manipulation of a grasped object requires contact with actuated components.

For each caging configuration q_{caging} in S_{caging}, the object contact subspace $CS_j(q_{caging})$ for the object and each actuated component AC_j can be determined by finding the object poses such that the object and component boundaries are coincident. The object-contact-space for the entire mechanism is then the intersection of the contact spaces $\bigcap_{j=1}^{P} CS_j$ calculated for the actuated components of interest. For the planar, underactuated hand designs investigated in this study, that space is comprised of configurations where the object makes contact with both fingers but not necessarily all finger links. For more complex hands, especially ones where not all actuated components necessarily need to contact the object during manipulation, the different permutations of actuated components would need to be considered.

C. Manipulable Cage

Instead of considering only rigid, immovable caging configurations, as is used in the conventional definition of caging, we propose the concept of a *manipulable cage* - caging configurations that can be reconfigured into other caging or non-caging configurations with some non-zero work. Relative to the commanded reference inputs, the work done by the actuators can be mapped to the corresponding object configuration satisfying the contact constraints of the manipulator [13]. Mahler et al. [16] have presented a similar concept called energy-bounded caging - configurations which effectively cage the object with the assistance of some external force, such as gravity. In both of these definitions, an escape path in the energy field can be computed for a caged object, and the energy expenditure necessary to free the object is calculated. In our approach, however, we propose utilizing an understanding of the energy profile of the possible object configurations in order to modulate the object motion within the hand.

For a given reference value a_k, either position p_A or rotation θ_A, the energy for the kth actuated component is:

$$E_{Ak}(p_k) = -F_{Ak}(p_k - p_{Ak}) \quad (1)$$

$$E_{Ak}(\theta_k) = -\tau_{Ak}(\theta_k - \theta_{Ak}) = -f_{Ak} r_{Ak}(\theta_k - \theta_{Ak}) \quad (2)$$

for actuation force f_A or actuation torque τ_A and corresponding transmission radius r_A. In the context of hands, we assume that actuated components (most commonly finger phalanxes) can only push, not pull, so configurations with negative energy values, indicating configurations where the actuator can achieve the reference input without the associated actuated components making contact with the object, are treated as zero-energy configurations. For simplicity, the effects of passive elements like return springs or flexural stiffness on the energy state are assumed to be negligible relative to the actuator energy and are disregarded.

The full system energy for each configuration is then the summation of the energy for all actuators:

$$E_A(a_{hand}) = \sum_{k}^{N} max(E_{Ak}(a_k), 0) \quad (3)$$

Under the assumptions of this model, each actuator is at its lowest energy configuration if it reaches its target commanded reference. In a multi-component system, interactions and interferences between components can make it impossible for each actuator to achieve its commanded reference. The system is expected to reconfigure toward the lowest energy configuration, of all the possible system configurations permitted by the components' geometries and respective workspaces.

Evaluating this for all hand-object configurations in turn produces an object energy field detailing the system reconfiguration behavior in response to the actuation inputs. In this way, each caging manipulation primitive can establish a particular region of attraction in the object workspace. These details can be numerically extracted from the object energy field to provide more insight regarding the grasp stiffness and the effective bias that the hand applies to the object pose [17].

D. Case Study

Fig. 4 presents an example object energy field, evaluated for a simple gripper, composed of a two-link underactuated finger and a static opposition thumb (Fig. 4a), manipulating a circlular object. The system energy across the object-contact space were evaluated for in increasing set of actuation reference values, and the plotted energy values (Fig. 4b) were normalized with respect to the maximum recorded system energy value. The model shows that, as expected, closing the finger pulls the object inwards, toward a y-value around 0.4 (the lighter regions in the plot), for an object with radius 0.175. By increasing the actuation input from 0.6 to 0.8, the lower-energy regions become smaller, indicating that the object is held in a more secure grasp. For actuation input 0.4, the smaller overall shaded region indicates that there are portions of the object-contact space where the reference position value for the actuator was not sufficient for the finger to close enough to make contact with the object.

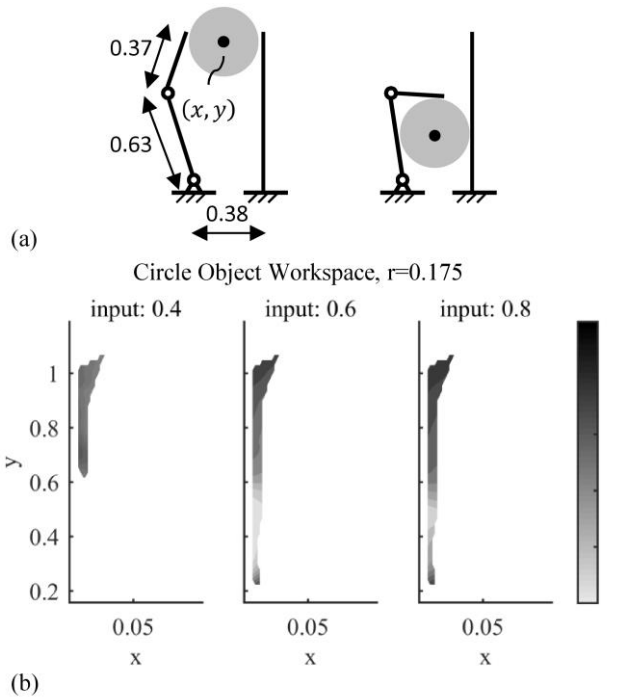

Fig. 4 – Object energy field for caging manipulation evaluated for a simple gripper utilizing a single two-link, underactuated finger and a static thumb. The input is the normalized actuator reference for the two-link finger.

III. Experimental Procedure

To evaluate this manipulation strategy experimentally, we explored the planar, caging-manipulation workspace for various object geometries (Fig. 5). The egg geometry was determined by a 25mm diameter circle and a 45mm diameter circle with a variable offset between the two. All objects were printed and had attachment points for fiducial markers. This paper focuses on results for the T42b hand, a tendon-driven design with a two-link underactuated finger and an opposing one-link thumb. The two fingers are each independently driven by a Dynamixel MX-28 smart servo. The design, detailed further in Fig. 6, is a variation of an underactuated design taken from the Yale OpenHand Project library [18]. To minimize friction, both the finger and object surfaces were 3D-printed on a Stratasys Fortus 250mc with ABSplus, with layers oriented in the same direction.

A Logitech C920 webcam was mounted above the test hand, which was fixtured in place. Aruco fiducial markers [19] were affixed to the test object centroid and ends of each finger link, via the revolute joint center where possible. Using Python and OpenCV for image capture and fiducial tracking, this setup could record at approximately 15 frames per second. For each commanded actuation input, the marker positions were tracked and recorded continuously throughout the motion. The object space reference frame was established at the midpoint between the two proximal finger joints.

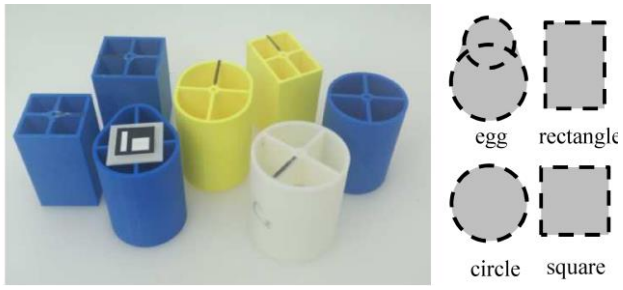

Fig. 5 - Various object geometries evaluated by the proposed caging manipulation experimental study.

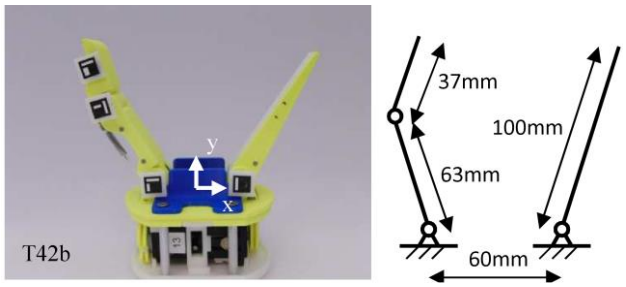

Fig. 6 – The T42b hand design used in this study. Aruco fiducial markers were attached to the object and finger joints, and a webcam was mounted above the test fixture to track the system behavior.

A. Actuation Space Exploration

To generate the viable actuation space for each object, we took advantage of underactuated hands' mechanical adaptability. Each actuator's operating range was first discretized, and for each actuator, it was driven to each discretized value via position-control. The opposing actuator was then commanded to close via a constant torque, and the actuator encoder values were recorded after the object and hand elements were fully constrained. This exploration excluded cases where the hand ejected the object during grasp acquisition or where the hand configuration was visually identified as a non-caging. The object was reset to the middle of the hand workspace between each grasp acquisition test. This sparse sampling of points in the actuator space was then interpolated to produce the set of actuator inputs used in the workspace evaluation.

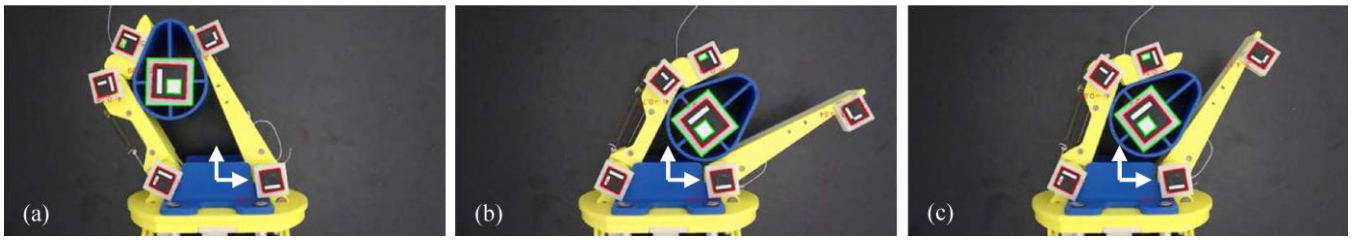

Fig. 7 – Summary of an evaluated motion trajectory: from an initial point in actuation space (a), the hand is commanded to the target point in actuation space (b), and after the motion concludes, an open-loop, torque-based squeezing operation is commanded to ensure contact.

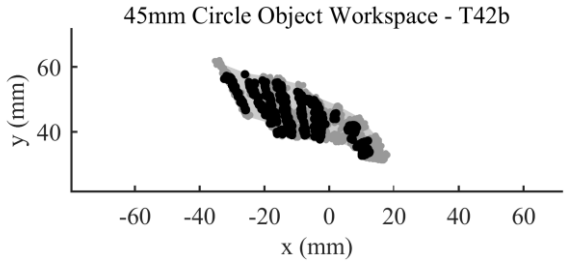

Fig. 8 – Experimental results for the circlular object geometry and the T42b.

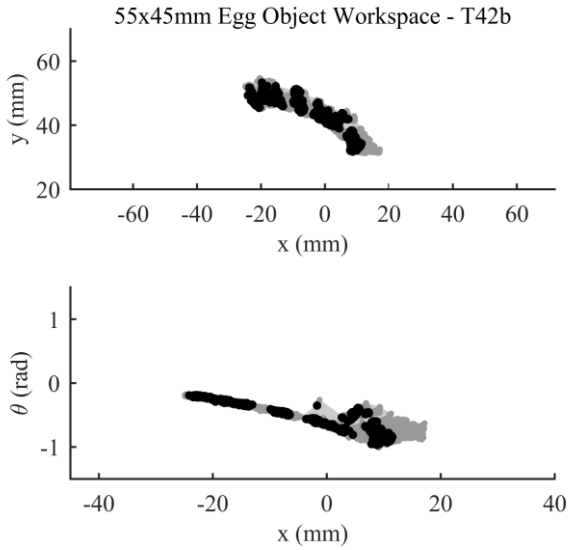

Fig. 9 – Experimental results for the egg object geometry and the T42b.

B. *Object Workspace Exploration*

The exploration procedure iterated through and tested all possible initial and target combinations of actuator inputs from the sampled actuation space. In order to account for contact variability and/or hysteresis in the pulley transmission, the actuators are initially driven to their target values in position-mode, and then switched to torque-mode to maximize contact. Fig. 7 summarizes these steps in a typical tested manipulation execution.

The actuation inputs calculated in the previous section are sufficient to keep the object within the grasp acquisition range and avoid ejection. As a result, each workspace exploration could be run continuously. A typical exploration of the full actuation space evaluates ~160 independent motion trajectories, lasting a total duration of 20 minutes. At least two full workspace exploration trials were completed for each unique hand-object combination.

IV. Experimental Results

A. *Manipulation Workspaces*

Examples of the object workspaces achievable through the proposed caging manipulation are shown in Fig. 8-9. The black points designate the final object grasp poses, and the grey points corresponds to all object poses during the execution of each caging manipulation move. The results for all the evaluated hand-object combinations are detailed further in Table II. The achievable object workspaces ranged from 29 to 46mm in the x-direction, 5 to 26mm in the y-direction, and up to 0.97 rad in total reorientation.

TABLE II
Caging Manipulation Evaluation – T42b

Object	range(x) (mm)	range(y) (mm)	range(θ) (rad)
50mm Circle	45.98	21.81	n/a
55×45mm Egg	44.90	25.24	0.973
45×30mm Rectangle	34.75	5.86	0.837
40mm Square	41.35	24.25	0.809
35mm Square	29.13	5.79	0.956

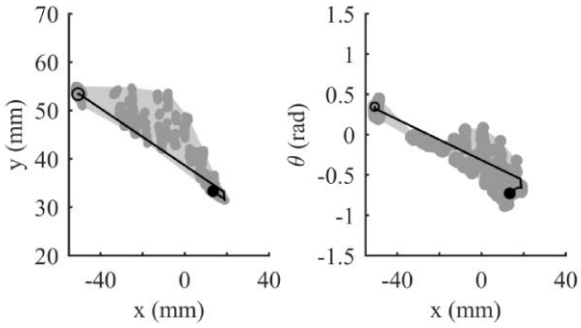

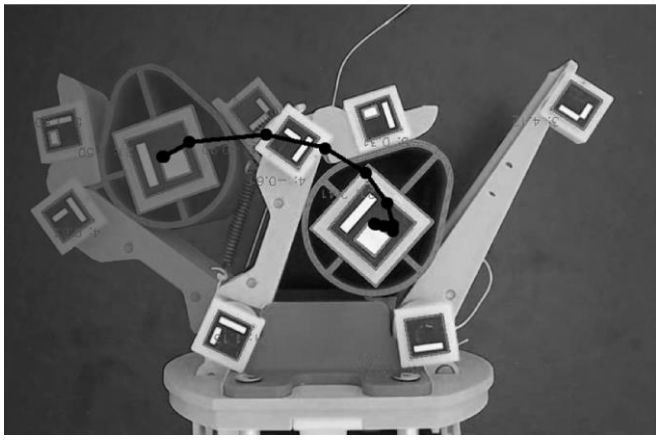

Fig. 10 – Example trajectory comparing the recorded fiducial data and the video. Trajectory in the video overlay were manually identified from frame grabs. Automatic fiducial detection failed when manipulation speed was too high, so recorded fiducial data lacks some of the trajectory details between the initial and final grasp poses.

As has been previously proposed in past work [13], [20], [21], the manipulation capability is determined by a combination of the hand's geometric design parameters and the object shape. In particular, the overall xy workspace was most limited for the rectangular and square objects, which were often aligned against the hand palm or a finger link.

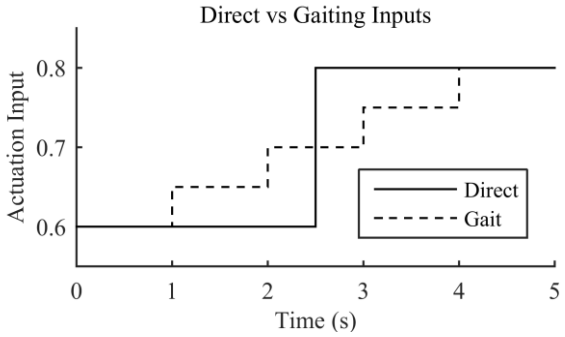

Fig. 11 – Summary of the difference in actuator inputs for a direct vs a gaited motion.

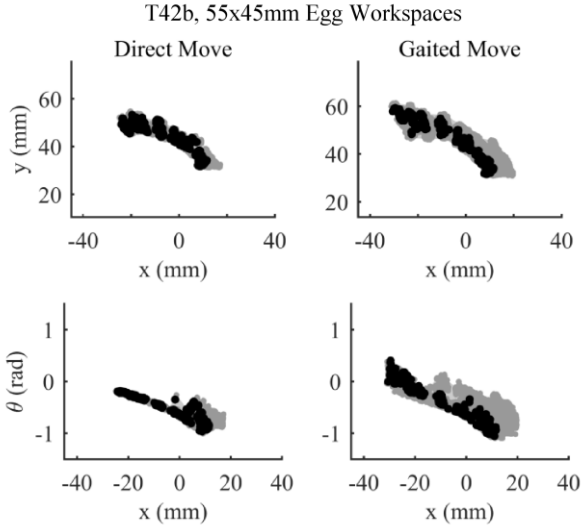

Fig. 12 – Comparison between the workspaces evaluated through direct actuator move commands vs. gaited actuator move commands.

The curved surfaces of the egg and circle geometries made them easier to reconfigure within a grasp and avoid line-contacts with the finger-links or palm, made evident by the increased xy and reorientation workspaces.

Figure 10 presents an example object trajectory for the 55×45mm egg object superimposed on the recorded hand-object workspace. This specific trajectory shows a substantial translation in the horizontal direction. To locate this trajectory within the dataset, we divided the recorded object motions into left and right movements, and sorted them into bins with respect to object displacement. Then, the trajectory with the largest horizontal translation was selected from the most populated bin. The evaluated object workspaces can be sampled to determine highly repeatable object trajectories that may be useful when planning manipulation strategies.

B. Gaiting and Regrasping

Formally, finger-gaiting and regrasping have been proposed as strategies to recycle or reset the workspace of the finger and/or other actuated components [1]. Both approaches can have strict requirements, as finger-gaiting requires a redundant set of fingers that can facilitate the disengagement and reengagement of a finger required for a stable grasp, and regrasping necessitates the ability to robustly release the object in the environment to attempt a new grasp. Mechanical hardware may not be sufficient to enable the former, and the task requirements may not permit the latter.

The caging attribute of the proposed manipulation primitives offers a hybrid solution. Caging enables limited object mobility, but to a sufficient degree for some subset of contacts to be completely disengaged. This helps overcome friction and allows the object some limited mobility mid-realignment while avoiding ejection.

This was evaluated by modifying the servo trajectory between commanded motions, as shown in Fig. 11. Instead of moving to the desired servo positions directly, the direct move is discretized into steps, and the two fingers alternate active motions. Qualitatively, this jostles the object within the grasp, as each finger effectively takes turns perturbing the object in a non-prehensile manner.

Fig. 12 shows an example of the object workspaces evaluated for direct and gaited actuator motion profiles. As contact is disengaged more frequently through gaiting, the dissipative effects from friction restrict the object motion less, and the hand can achieve a larger object workspace, in terms of both the final grasped object poses (black points) and the intermediate object poses during the execution of the manipulation primitive (grey region). Despite the uncoordinated breaks in contact, the object remained constrained to the hand workspace, albeit only demonstrated here for the simplified planar case. These examples suggest that a repeated and properly bounded release-and-regrasp gait can help compensate for the effects of friction due to unknown material properties.

V. CONCLUSION

In this paper, we analyzed *caging manipulation,* a manipulation primitive, which could be also be described as in-hand fumbling or shuffling. The caging characteristic allows for open-loop trajectories that avoid object ejection or loss of grasp without detailed knowledge of the contact conditions. This manipulation primitive was evaluated on a physical test setup for a set of object geometries and a planar, underactuated hand design with two-actuators. The experimental results showed that simple, open-loop actuator commands were sufficient to robustly manipulate objects within the hand workspace. Examples of open-loop gaiting motions, made possible by caging, were also demonstrated as a means of extending the manipulation workspace and compensating for different coefficients of friction. This may run counter to past, traditional approaches to dexterous manipulation, which requires object stability and well-maintained contact conditions within the grasp at all instances of the executed task.

While the proposed caging manipulation primitive can be applied on any hand design, it is particularly useful in underactuated hands, which are typically designed to passively cage around the object, regardless of the particularities of its geometry. Caging manipulation extends the underactuated hand's passive adaptation and applies a bias to the object, constrained to its allowable workspace relative to the hand. We hope that the robustness

demonstrated by the experimental examples will encourage researchers to consider other manipulation primitives that relax grasp constraints where possible to enable more functionality in other useful ways.

REFERENCES

[1] Z. Li, P. Hsu, and S. Sastry, "Grasping and coordinated manipulation by a multifingered robot hand," *Int. J. Rob. Res.*, vol. 8, no. 4, pp. 33–50, 1989.

[2] M. T. Mason and J. K. Salisbury, *Robot hands and the mechanics of manipulation*. 1985.

[3] M. Grebenstein, M. Chalon, W. Friedl, S. Haddadin, T. Wimbock, G. Hirzinger, and R. Siegwart, "The hand of the DLR Hand Arm System: Designed for interaction," *Int. J. Rob. Res.*, vol. 31, no. 13, pp. 1531–1555, Nov. 2012.

[4] T. Senoo, Y. Yamakawa, S. Mizusawa, A. Namiki, M. Ishikawa, and M. Shimojo, "Skillful Manipulation Based on High-speed Sensory-Motor Fusion," in *International Conference on Robotics and Automation*, 2009, pp. 1611–1612.

[5] G. Vassura and A. Bicchi, "Whole-Hand Manipulation: Design of an Articulated Hand Exploiting All Its Parts to Increase Dexterity," in *Robots and Biological Systems: Towards a New Bionics?*, 1993, pp. 165–177.

[6] L. U. Odhner, R. R. Ma, and A. M. Dollar, "Open-loop precision grasping with underactuated hands inspired by a human manipulation strategy," *IEEE Trans. Robot.*, vol. 10, no. 3, pp. 625–33, 2013.

[7] M. N. Ahmadabadi and E. Nakano, "A "constrain and move" approach to distributed object manipulation," *IEEE Trans. Robot. Autom.*, vol. 17, no. 2, pp. 157–172, 2001.

[8] W. Wan, R. Fukui, M. Shimosaka, T. Sato, and Y. Kuniyoshi, "Grasping by caging: A promising tool to deal with uncertainty," in *International Conference on Robotics and Automation*, 2012, pp. 5142–5149.

[9] S. Makita and Y. Maeda, "3D multifingered caging: Basic formulation and planning," in *International Conference on Intelligent Robots and Systems*, 2008, pp. 2697–2702.

[10] R. Diankov, S. S. Srinivasa, D. Ferguson, and J. Kuffner, "Manipulation planning with caging grasps," in *IEEE-RAS International Conference on Humanoid Robots*, 2008, pp. 285–292.

[11] a. Rodriguez, M. T. Mason, and S. Ferry, "From caging to grasping," *Int. J. Rob. Res.*, vol. 31, no. 7, pp. 886–900, Apr. 2012.

[12] A. Sudsang, J. Ponce, and N. Srinivasa, "Algorithms for Constructing Immobilizing Fixtures and Grasps of Three-Dimensional Objects," no. 2.

[13] G. A. Kragten and J. L. Herder, "The ability of underactuated hands to grasp and hold objects," *Mech. Mach. Theory*, vol. 45, no. 3, pp. 408–425, 2010.

[14] A. Rodriguez, M. T. Mason, and S. S. Srinivasa, "Manipulation Capabilities with Simple Hands," *Exp. Robot.*, pp. 1–15, 2014.

[15] A. Blake, "Caging 2D Bodies by 1-Parameter Two-Fingered Gripping Systems," in *IEEE International Conference on Robotics and Automation*, 1996, no. April, pp. 1458–1464.

[16] J. Mahler, F. T. Pokorny, Z. Mccarthy, A. F. Van Der Stappen, and K. Goldberg, "Energy-Bounded Caging : Formal Definition and 2D Energy Lower Bound Algorithm Based on Weighted Alpha Shapes," in *International Conference on Ro*, 2016.

[17] T. Yamada, T. Koishikura, Y. Mizuno, N. Mimura, and Y. Funahashi, "Stability Analysis of 3D Grasps by A Multifingered Hand," in *International Conference on Robotics and Automation*, 2001, pp. 2466–2473.

[18] R. R. Ma, L. U. Odhner, and A. M. Dollar, "A Modular, Open-source 3D Printed Underactuated Hand," in *International Conference on Robotics and Automation*, 2013, pp. 2737 – 2743.

[19] S. Garrido-Jurado, R. Munoz-Salinas, F. J. Madrid-Cuevas, and M. J. Marin-Jimenez, "Automatic generation and detection of highly reliable fiducial markers under occlusion," *Pattern Recognit.*, vol. 47, no. 6, pp. 2280–2292, 2014.

[20] D. M. Aukes, B. Heyneman, J. Ulmen, H. Stuart, M. R. Cutkosky, S. Kim, P. Garcia, and A. Edsinger, "Design and testing of a selectively compliant underactuated hand," *Int. J. Rob. Res.*, Feb. 2014.

[21] L. U. Odhner, R. R. Ma, and A. M. Dollar, "Exploring Dexterous Manipulation Workspaces with the iHY Hand," *J. Robot. Soc. Japan*, vol. 32, no. 4, pp. 318–322, 2014.